The Journal of Experimental Biology 204, 3283–3294 (2001)
Printed in Great Britain © The Company of Biologists Limited 2001
JEB3623

Speeds and wingbeat frequencies of migrating birds compared with calculated benchmarks

C. J. Pennycuick

School of Biological Sciences, University of Bristol, Woodland Road, Bristol BS8 1UG, UK

(e-mail: colin@pennycuick.u-net.com)

Accepted 9 July 2001

Summary

Sixteen species of birds passing Falsterbo in southwest Sweden during the autumn migration season were observed using short-range optical methods. Air speeds and wingbeat frequencies were measured, reduced to sea level, and compared with benchmark values computed by Flight.bas, a published flight performance program based on flight mechanics. The benchmark for air speed was the calculated sea-level value of the minimum power speed (V_{mp}). The mean speeds of three raptor species that flew by flap-gliding were below V_{mp}, apparently because the flap-glide cycle involved slowing down below V_{mp} when gliding and accelerating back up to V_{mp} when flapping. The mean speeds of 11 species that flew by continuous flapping were between $0.82V_{mp}$ and $1.27V_{mp}$. Two passerine species that flew by bounding had mean speeds of $1.70V_{mp}$ and $1.96V_{mp}$, but these high mean speeds reflected their ability to fly faster against head winds. These results do not support predictions from optimal migration theory, which suggest that migrating birds 'should' fly faster, relative to V_{mp}. However, observations were restricted for technical reasons to birds flying below 200 m and may not represent birds that were seriously committed to long-distance migration.

The benchmark wingbeat frequency (f_{ref}) was derived from dimensional reasoning, not from statistical analysis of observations. Observed wingbeat frequencies ranged from $0.81f_{ref}$ to $1.05f_{ref}$, except in the two bounding species, whose wingbeat frequencies appeared anomalously high. However, the mechanics of bounding with a power fraction q imply that gravity during the flapping phase is increased by a factor $1/q$, and when the value of gravity was so adjusted in the expression for f_{ref}, the wingbeat frequencies of the two bounding species were predicted correctly as a function of the power fraction. In small birds with more muscle power than is required to fly at speeds near V_{mp}, bounding is an effective method of adjusting the specific work in the muscle fibres, allowing conversion efficiency to be maximised over a wide range of speeds.

Key words: flight, bird, migration, wingbeat frequency, benchmark.

Introduction

Optimal air speeds

Hedenström and Alerstam (Hedenström and Alerstam, 1995) argued that different optimal air speeds can be identified for a migrating bird depending on whether the 'currency' that the bird is trying to maximise is distance per unit fuel energy used, average speed over one or several flight stages and stopovers, or various other possibilities. On the other hand, Alerstam and Hedenström (Alerstam and Hedenström, 1998) conceded that it is difficult in practice to determine whether a migrating bird is attempting to maximise one currency rather than another, by comparing the observed speed with alternative theoretical optimal speeds. Not the least of the difficulties is that, to estimate the theoretical speeds, a curve of power *versus* speed must first be calculated for the bird. This requires some morphological data, which are never available for each individual bird observed in the field. Species means can be used but, in the case of radar observations, even the species is often doubtful. Even when accurate data are available for body mass and wing measurements, as in the case of a bird flying in a wind tunnel, the exact shape of the power curve at high speeds is poorly known. Recognising that this is critical for estimating optimum speeds, Alerstam (Alerstam, 2000) suggested a way in which the power curve might be modified to cover higher speeds, but more experimental evidence is needed before a revised model could be used with confidence.

Calculated benchmarks

The objective of the present project is to establish physical 'benchmarks' against which the performance of wild birds can be measured, without any hypothesis as to the expected values at which birds 'should' fly. The basis for calculating the benchmarks, including assumptions made and values currently assumed for variables, is the Basic program Flight.bas, which is published on the internet (http://detritus.inhs.uiuc.edu/wes/

pennycuick.html) and runs under QBasic. Flight.bas is based on flight mechanics (not statistics) and implements the physical model described by Pennycuick (Pennycuick, 1975; Pennycuick, 1989), which is itself adapted from classical aeronautics. Where experimental results do not agree with the program's predictions, Flight.bas allows the source of the discrepancy to be traced, so as to amend the values assumed for variables that cannot be measured directly. For example, Pennycuick et al. (Pennycuick et al., 1996b) showed that the minimum power speed (V_{mp}) can be inferred empirically from measurements of wingbeat frequency in birds flying in a low-turbulence wind tunnel, and they used this as a check on the value of V_{mp} predicted by Flight.bas. The measured and calculated values of V_{mp} agreed in two very different birds, a thrush-nightingale (*Luscinia luscinia*, Turdidae) and a teal (*Anas crecca*, Anatidae), when the body drag coefficient C_{Db} was set to 0.08, but the program under-estimated V_{mp} when early, much higher, estimates were used for C_{Db}. These anomalously high values, ranging from 0.25 to 0.40, were obtained by measuring the drag of frozen, wingless bird bodies and were already known to be due to massive flow separation, which does not appear to occur in living birds. This observation increases the confidence with which calculated values of V_{mp} can be used for comparison with speeds observed in the field. Using too high a value for C_{Db} causes the minimum power speed to be underestimated and creates the illusion that wild birds fly at a higher multiple of V_{mp} than they actually do.

Selected benchmarks for air speed and wingbeat frequency

V_{mp} was selected as the benchmark air speed, not because any bird is expected to fly at this speed when migrating, but because it is the only speed on the power curve for which calculated values have some experimental backing (above). Also, Lighthill (Lighthill, 1977) pointed out that V_{mp} is the lower boundary of the range of speeds available for cruising powered flight and that prolonged powered flight is not practicable at lower speeds. The reasons for this are mechanical (not physiological) and were further elaborated by Pennycuick (Pennycuick, 1997). V_{mp} was calculated for each species from the following formula, which is adapted from Pennycuick (Pennycuick, 1975) and used in Flight.bas:

$$V_{mp} = 0.807k^{0.25}m^{0.5}g^{0.5}/[\rho_{SL}{}^{0.5}b^{0.5}(S_bC_{Db})^{0.25}], \quad (1)$$

where m is the body mass, g is the acceleration due to gravity, b is the wing span, S_b is the frontal area of the body, C_{Db} is the drag coefficient of the body and k is the induced power factor. Setting the air density to a fixed value ρ_{SL}, corresponding to sea level in the theoretical standard atmosphere, leads to a calculated 'equivalent' value for V_{mp}. 'True' air speeds, observed in the field, have to be 'reduced to sea level' (see below) before they can be compared with the value calculated from equation 1.

The benchmark wingbeat frequency (f_{ref}) was calculated from the formula:

$$f_{ref} = m^{3/8}g^{1/2}b^{-23/24}S^{-1/3}\rho_{SL}{}^{-3/8}, \quad (2)$$

where S is the wing area as defined by Pennycuick (Pennycuick, 1999). Like the value of V_{mp} calculated from equation 1, f_{ref} is an equivalent sea-level value because it is based on the sea-level air density (ρ_{SL}). Like equation 1, this formula contains physical variables only. It was derived by Pennycuick (Pennycuick, 1990) from dimensional reasoning, and modified by Pennycuick (Pennycuick, 1996a) in the light of field observations of wingbeat frequencies.

Requirements for field data

To obtain field data for comparison with the benchmarks, a stream of migrating birds is required, each one of which can be identified to a species for which measurements of body mass, wing span and wing area are available. This requirement restricts observation to sites and seasons where the topography causes a migration stream to concentrate and where migrants are flying low enough for visual identification. This, unfortunately, loses the advantage of tracking-radar observations, in which high-flying birds that are definitely committed to long-distance flight can be observed. By observing only low-level flight, it is difficult to be sure which birds are on their way to some distant destination and which are foraging locally or pausing in the study area *en route* to somewhere else. By selecting an area known to be a concentration point for migration, it is to be hoped that at least some of the birds observed were migrating, which was not the case in earlier projects using similar methods (Pennycuick, 1990; Pennycuick, 1996a). Besides allowing every bird to be visually identified, short-range, optical methods of observation have the important advantage that the wind can be measured immediately after each observation of speed. This provides much better time resolution than is possible by tracking balloon ascents, at intervals of hours, as is usually the only option in radar observations. Also, the wind can be measured at a point close to where the bird is flying.

Materials and methods

Study site and period

Birds were observed from 3 to 15 October 2000 from a vantage point opposite Falsterbo lighthouse, on the edge of the dunes (55°23.015′N, 12°48.917′E). The Falsterbo peninsula, at the southwestern point of Sweden, is a concentration area for migrants of many species leaving Sweden in the autumn. Karlsson (Karlsson, 1992) described the area and the research carried out there since the establishment in 1955 of a bird-ringing station at the lighthouse, and also summarised the numbers and timing of different bird species migrating through the area. Measurements of body mass, wing span and wing area are listed for the 16 study species in Table 1. These measurements came from the database summarised by Pennycuick (Pennycuick, 1999) or from later additions to that database, except that data for *Columba palumbus* had to be taken from Greenewalt (Greenewalt, 1962) because no original measurements were available.

Table 1. *Wing measurements of the study species and numbers of speed runs and video recordings obtained for each*

Species		Mass (kg)	Wing span (m)	Wing area (m^2)	Speeds (*N*)		Video (*N*)	
					Runs	Observations	Records	Wingbeats
Corvus corone	Hooded crow	0.553	0.925	0.147	20	46	2	50
Sturnus vulgaris	Starling	0.0884	0.384	0.0251	11	13	20	1157
Fringilla coelebs	Chaffinch	0.0228	0.262	0.0130	101	213	12	146
Buteo buteo	Common buzzard	0.964	1.29	0.254	58	210	16	1003
Accipiter nisus	Sparrowhawk	0.196	0.611	0.0642	21	47	3	119
Milvus milvus	Red kite	0.851	1.50	0.304	41	209	8	403
Ardea cinerea	Grey heron	1.21	1.60	0.358	61	333	3	278
Cygnus olor	Mute swan	9.01	2.31	0.682	25	107	2	98
Anas penelope	Wigeon	0.770	0.822	0.0829	7	11	9	580
Somateria mollissima	Eider	1.39	0.978	0.131	2	2	34	1029
Phalacrocorax carbo	Cormorant	2.56	1.35	0.224	38	88	24	2064
Columba palumbus	Wood pigeon	0.495	0.751	0.0797	19	31	8	200
Larus ridibundus	Black-headed gull	0.280	0.963	0.0985	9	17	1	20
Larus canus	Common gull	0.364	1.10	0.138	40	164	6	520
Larus argentatus	Herring gull	0.925	1.35	0.200	112	444	2	166
Larus marinus	Great black-backed gull	1.51	1.66	0.290	88	398	7	493

Ground speed measurements

Two methods were used to measure the ground speeds of passing birds.

(i) The Leica Vector is a pair of 7×42 binoculars with a built-in laser rangefinder and also a magnetic sensor that determines the direction in which the binoculars are pointing and a gravity sensor that determines the elevation angle. Built-in compensator magnets for the azimuth sensor can be adjusted by an automatic system, when the instrument is set up, to cancel local magnetic disturbances. In use, the instrument is aimed at a target, with the help of crosshairs in the centre of the field, and a button is pressed. The rangefinder measures the distance and sends the result, followed by readings from the azimuth and elevation sensors, *via* a serial output port. An error message is sent if the rangefinder fails to detect the returning light pulse. The Vector worked well on large, light-coloured birds, flying steadily along at distances of 100–600 m from the observer, but was seldom able to generate range measurements on small birds.

The nominal precision of the range reading, output by the Vector, was ±0.5 m. Repeated ranging of static targets resulted in standard deviations from zero at 398 m (20 measurements, all the same) to ±0.37 m at 149 m. The same standard deviation (±0.24 m) was measured at both 92 m and 779 m. The repeatability of the range measurement was thus better than the wing spans of most of the species in the study (Table 1). The nominal precision of the two angular encoders was 10^{-4} rad (0.0057 °). Standard deviations varied from 0.10 to 0.14 ° in azimuth and from 0.050 to 0.073 ° in elevation. These values are a realistic indication of the Vector's precision in use because a range reading could not be obtained unless the instrument was accurately aligned on the bird. An angular error of ±0.2 ° at a range of 500 m would correspond to a positional error of ±1.7 m, but the repeatability on static targets was better than this. Attempts were made to induce errors in the gravity sensor by rotating the instrument with sudden starts and stops, but no errors were detected. To minimise such effects, the instrument was mounted on a heavy Gitzo photographic tripod, with a fluid-damped pan-tilt head intended for use with video cameras, giving very smooth rotation.

(ii) The ornithodolite measures distance with an optical coincidence rangefinder of 25 cm base and the azimuth and elevation angles with eight-bit optical encoders. This instrument, and its calibration and precision, were described by Pennycuick (Pennycuick, 1982a). A new interface was built for the present project, based on a PIC 16C74 microcontroller, which read the sensors when the button was pressed and output the readings in serial form. The ornithodolite was used to track small birds at distances of 50–120 m from the observer.

Whichever instrument was in use, the data were sent to the serial port of a laptop computer (MBC Proteus) and were read, together with the time from the computer's real-time clock, by a program written in Microsoft QBasic. The 'tick' period of the clock was found by experiment to be 54.925 ms, an improvement on the earlier ornithodolite interface, whose time resolution was 100 ms. The data were transformed from polar to cartesian coordinates (as described by Pennycuick, 1982b) and recorded as timed, three-dimensional points in space. As in previous ornithodolite projects, a 'run' was defined as a series of two or more such points, and an 'observation' was the measurement of ground speed (horizontal and vertical) obtained by comparing each point with the previous one. The number of observations in each run was therefore one less than the number of points. The numbers of runs and observations for each of the 16 study species are shown in Table 1. The data were saved in the field onto hard disc and were in the same format irrespective of whether the Vector or the ornithodolite was the source of the data.

Wind measurement

The anemometer hardware consisted of a whirling-cup and

vane assembly from Maplin Electronics, fitted with optical encoder discs, home-made from lith film. Wind direction was measured with a seven-bit angular encoder, Gray-coded in steps of 5°. Wind speed was measured with a 36-segment continuously rotating disc by counting the sectors passing an optical sensor in a fixed period. The wind speed sensor was calibrated in the Lund wind tunnel (Pennycuick et al., 1997) to give true (not equivalent) air speed in $m\,s^{-1}$. Both sensors were read by a PIC 16C71 microcontroller, which sent the readings at intervals of 2.3 s *via* a UHF radio link to a receiver, which was connected to a second serial port on the computer (Socket S-I/O). This port was activated by the controlling program whenever a run was completed and saved. The wind speed and direction were automatically received and recorded as part of the data for the run.

The anemometer assembly was mounted on a mast 3 m above the ground. The radio link eliminated the need for an anemometer cable, so that the mast could be positioned clear of any upwind obstructions. Apart from the lighthouse garden, which supported a stand of trees, the immediate surroundings were a flat and relatively unobstructed golf course on the east and south sides, and the waters of Öresund to the west and north. There were no hills in any direction high enough to cause wind disturbances. As the birds' flying heights were within 200 m of the surface, no correction was needed to the wind direction, but the wind speed was corrected according to the conventional wind gradient equation:

$$V_{h2} = V_{h1}[\ln(h_2/h_r)/\ln(h_1/h_r)], \quad (3)$$

where V_{h2} is the wind speed at the bird's flying height (h_2), V_{h1} is the measured wind speed at the anemometer, whose height is h_1, and h_r is a 'roughness height', which can be assigned a value of between 10^{-4} m for a glassy-smooth surface to 10^{-2} m for a very rough surface (Sutton, 1953). A 'medium' value of 10^{-3} m was used throughout for h_r. The whirling-cup type of anemometer measures true (not equivalent) wind speed which, after correction for the flying height, was vectorially subtracted from the measured ground speed to give an estimate of the true air speed. Wind speeds, corrected to flying height, varied from 0 to 14.3 $m\,s^{-1}$.

Wingbeat frequency

Analogue video was recorded in the field with a Panasonic NV-S7B camcorder on S-VHS-C tape cassettes, in the European PAL format, in which 50 'fields', each with half the number of horizontal lines of the full 'frame', are recorded per second, at equal time intervals of 20 ms. Wingbeat frequencies were measured from a copy of the original tape, in which the individual fields were numbered (Pennycuick, 1996a). Each sequence of wingbeats was played back in slow motion, or single-stepped one field at a time, beginning and ending the sequence at the same point in the wingbeat cycle. The time for the sequence, and hence the frequency, was found from the numbers of the first and last fields. The standard deviation of wingbeat frequency was estimated by first finding the mean and standard deviation of its reciprocal, the wingbeat period. The reason for this, and the method of calculation, were explained by Pennycuick (Pennycuick, 1990).

In the case of steady flapping flight, several flapping sequences could often be measured end to end, each sequence beginning at the field where the previous sequence ended. As in previous studies, the preferred point in the cycle for beginning and ending each sequence was the moment at the beginning of the downstroke when the wings come under load. This transition is abrupt and can be identified in views from different directions. However, in flap-gliding and bounding flight, some birds tended to begin a sequence with a partial downstroke from the gliding position, and it was found more practical to use the 'fully down' position for beginning and ending a flapping sequence. Because of this, the time from the first to the last fully down point of a sequence was shorter by one wingbeat period than the true duration of the sequence, and this had to be allowed for when measuring the 'power fraction' in flap-gliding or bounding flight, i.e. the proportion of the time spent in flapping. The 'wingbeat frequency' in these intermittent flight styles refers to the frequency within a sequence of continuous flapping, not to the average over flapping and non-flapping periods. The numbers of records obtained and wingbeats counted are shown for each of the 16 study species in Table 1.

Data reduction

Both air speed and wingbeat frequency are expected to be functions of the air density, whose measured value ρ varied from one run to another. The air density at the observer's position was first found from the ambient air temperature and barometric pressure and then corrected for the measured height difference between the observer and the bird. The formulae for these operations were given by Pennycuick (Pennycuick, 1999). The air density at sea level in the standard atmosphere was assigned a fixed value (ρ_{SL}) of 1.23 $kg\,m^{-3}$. σ is defined as the ratio of the ambient to the standard air density:

$$\sigma = \rho/\rho_{SL}. \quad (4)$$

Following aeronautical convention, observations of air speed and wingbeat frequency were 'reduced' to the values that would have prevailed at sea level, according to theoretical expectations, before comparisons were attempted. As air speed is expected to vary inversely with the square root of the air density (equation 1), the measured 'true' air speed (V_t) was reduced to the 'equivalent' sea-level air speed (V_e) thus:

$$V_e = V_t\sqrt{\sigma}. \quad (5)$$

An equivalent wingbeat frequency (f_e) was obtained likewise by reducing the measured true wingbeat frequency (f_t) to the sea-level value. As wingbeat frequency is expected to vary inversely with the 3/8 power of the air density (equation 2), the reduction equation in this case is:

$$f_e = f_t\sigma^{3/8}. \quad (6)$$

The effect of reducing the data to sea level was small because the air density at flying height varied only from 1.19 to 1.26 $kg\,m^{-3}$, giving values of σ of 0.98–1.02. These reductions

Table 2. *Observed and calculated speeds and wingbeat frequencies*

Species	Equivalent air speed ($m s^{-1}$)		Wingbeat frequency (Hz)	
	Observed	V_{mp}	Observed	f_{ref}
Corvus corone	10.5±2.03	12.1±0.976	3.84±0.0522	4.74±0.181
Sturnus vulgaris	17.3±1.75	10.2±0.864	10.6±1.25	9.97±0.385
Fringilla coelebs	15.3±3.46	7.82±0.715	18.2±1.74	10.8±0.691
Buteo buteo	9.31±1.92	12.3±1.21	3.63±0.168	3.54±0.218
Accipiter nisus	8.72±2.40	10.5±1.03	5.10±0.321	6.30±0.388
Milvus milvus	7.90±1.81	10.9±1.08	2.88±0.0926	2.75±0.170
Ardea cinerea	11.0±1.66	11.9±1.17	2.90±0.0354	2.79±0.172
Cygnus olor	16.0±0.700	19.4±2.08	3.38±0.0863	3.37±0.264
Anas penelope	17.1±1.99	14.3±1.41	6.83±0.330	7.27±0.500
Somateria mollissima	20.2±3.51	15.9±2.19	6.47±0.294	6.60±0.586
Phalacrocorax carbo	15.0±1.80	16.6±1.39	4.83±0.156	5.09±0.265
Columba palumbus	15.4±2.06	12.9±1.27	5.61±0.256	6.81±0.420
Larus ridibundus	10.1±1.89	9.42±0.964	3.27±0.0110	4.04±0.274
Larus canus	11.6±1.74	9.62±0.946	2.98±0.151	3.50±0.216
Larus argentatus	11.8±2.07	11.9±1.06	3.13±0.0761	3.61±0.218
Larus marinus	12.8±1.31	12.6±1.35	2.91±0.223	3.14±0.215

Numbers after the ± symbols are standard deviations of observed quantities and uncertainties of calculated quantities (N=6).
V_{mp}, minimum power speed; f_{ref}, calculated equivalent wingbeat frequency.

would have a larger effect in a situation where birds were observed over a wider range of heights, as in tracking-radar studies. In that case (and also, in principle, in the present project), unreduced observations are not comparable either with a reference value calculated for a fixed height or with each other.

Results

Calculated and observed values

Table 2 shows the mean observed equivalent air speeds and wingbeat frequencies for each of the 16 study species, together with estimates for the minimum power speed (V_{mp}) for each species calculated from equation 1 and the reference wingbeat frequency (f_{ref}) from equation 2. Values of the morphological variables for each species are given in Table 1, and the values used for the other variables in equations 1 and 2 and their assumed uncertainties are given in Table 3.

In Fig. 1 and Fig. 2 the observed mean values of air speed and wingbeat frequency are compared with the benchmark values calculated for each species from equations 1 and 2, by plotting the ratio of the observed to the calculated value, on a horizontal scale. The observed values are the means of samples and are accompanied in Table 2 by standard deviations, but the benchmark values were obtained directly from the measurements in Table 1 and Table 3. These estimates do not have standard deviations as such, as they are not sample statistics, but each does have an 'uncertainty'. This results from the uncertainties of the values used for the individual variables on the right-hand side of equations 1 and 2, each of which contributes to the uncertainty of the result on the left-hand side. The uncertainties of V_{mp} and f_{ref} were calculated by the method of Spedding and Pennycuick (Spedding and Pennycuick, 2001) and are listed in Table 2. The procedure is conventional in the physical sciences, but is based on a different principle from the calculation of the standard deviation of a sample. It would be out of order to use these uncertainty estimates in statistical tests of significance as they do not satisfy the assumptions underlying tests of this type. There is, in any case, no starting hypothesis as to the speeds at which birds 'should' fly, which could be rejected by a test of significance.

Table 3. *Assumed values for variables used in the calculations and their uncertainties expressed as a proportion of the value*

Variable	Symbol	Value	Uncertainty
Induced power factor	k	1.2	0.2
Body drag coefficient	C_{Db}	0.10	0.2
Acceleration due to gravity ($m s^{-2}$)	g	9.81	0.01
Sea-level air density ($kg m^{-3}$)	ρ_{SL}	1.23	Fixed value

Flight style

Three different flight styles could be distinguished, continuous flapping (most species), flap-gliding and bounding. The three raptor species in the sample invariably flew by flap-gliding, i.e. by alternately flapping and gliding for short periods. The chaffinch (*Fringilla coelebs*) invariably flew by bounding, i.e. by alternately flapping for a few wingbeats, then free-falling with the wings closed, while the starling (*Sturnus vulgaris*) sometimes flew by bounding and sometimes by continuous flapping. Starlings were not seen flap-gliding, either visually or on video.

Equivalent air speed

The species have been arranged in Fig. 1 in descending order of their 'relative air speeds', meaning the ratio of the observed mean equivalent air speed to the calculated minimum

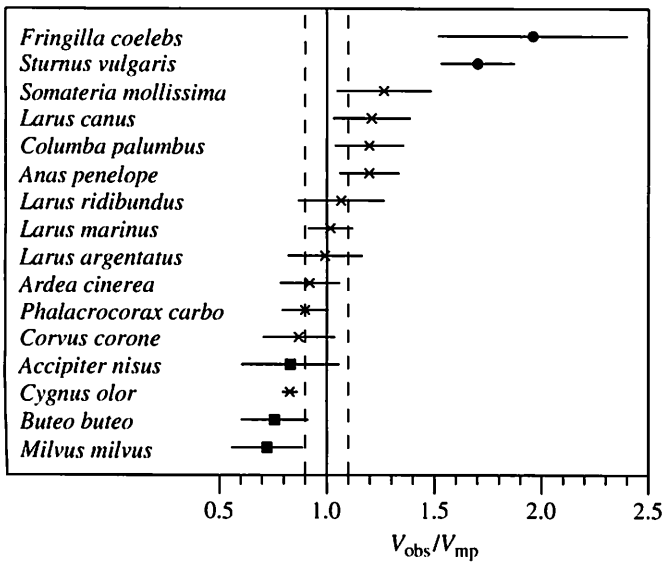

Fig. 1. Observed equivalent air speed (V_{obs}), with horizontal standard deviation bars, normalised by dividing by the calculated minimum power speed (V_{mp}). Squares are for species that flew by flap-gliding, crosses for flapping and circles for bounding. Data from Table 2.

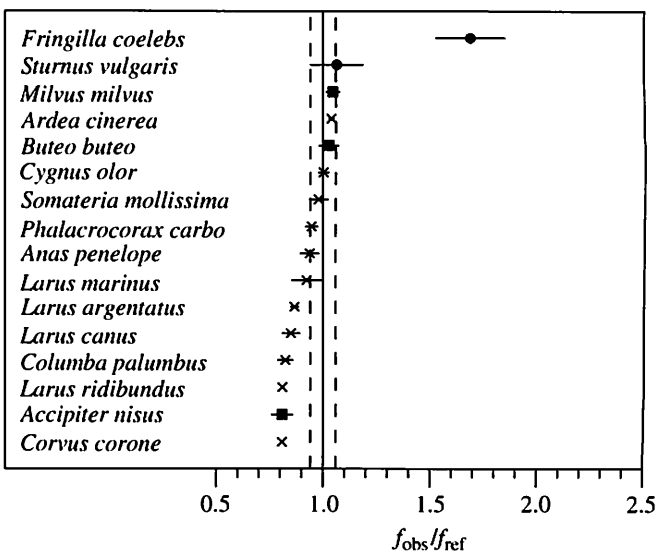

Fig. 2. As Fig. 1, but showing the ratio of observed to calculated equivalent wingbeat frequency (f_{obs}/f_{ref}). Data from Table 2.

power speed, both from Table 2. A relative airspeed of 1 (solid vertical line) means that the observed mean speed was equal to the calculated value of V_{mp}. The uncertainty of V_{mp}, also given in Table 2, varied in different species, ranging from 8 to 12% of the calculated value, which is indicated approximately by the vertical dashed lines at 0.90 and 1.10. Different symbols have been used in Fig. 1 to classify the styles of flight used by each species. Crosses signify species that flew by continuous flapping flight, and these dominate the middle part of Fig. 1, with observed relative air speeds between 0.83 and 1.27. The three species that flew by flap-gliding (squares) are clustered at the bottom of the table, with relative air speeds down to 0.73, while the two species that flew by bounding (circles) are at the top, with mean air speeds up to nearly twice V_{mp}.

Wind effect

A 'tail wind' is conventionally defined as the scalar difference between ground speed and true air speed. The magnitude of this difference represents the extent to which the wind helps or hinders the bird, regardless of whether the wind is aligned with the bird's heading or at an angle to it. The 'wind effect' means that a bird whose ground speed is less than its air speed will normally respond by increasing its air speed, resulting in a negative correlation between the air speed and the 'tail wind' so defined (Pennycuick, 1982b). Fig. 3 shows such graphs for three species with different flight styles. The chaffinch showed a very strong wind effect, with air speeds from 8.64 m s^{-1} (1.1V_{mp}) to 24.3 m s^{-1} (3.1V_{mp}), which was the highest speed measured in any species in this study, either absolute or relative to V_{mp}. The high mean speed of the chaffinch (1.96V_{mp}) reflects its wide speed range and its ability to increase its speed when flying against head winds. The fitted line in Fig. 3A intersects zero wind (vertical dashed line) at an air speed only just above V_{mp}. In the common buzzard (*Buteo buteo*), which flew by flap-gliding, nearly all the speed observations were below the estimated minimum power speed, whereas in the cormorant (*Phalacrocorax carbo*), which flew by flapping, most were below V_{mp} but some were above. The correlation coefficient was negative and highly significant ($P \ll 0.01$) in each of these three species, although some other species in which sample numbers were small did not show a significant correlation.

Wingbeat frequency

In Fig. 2, the species have been arranged in descending order of the 'relative wingbeat frequency' for each species, i.e. the ratio of the observed equivalent wingbeat frequency to the calculated value of f_{ref} from Table 2. As in Fig. 1, the two bounding species (circles) occupy the top two places. The chaffinch was the only species whose observed wingbeat frequency was much higher than the calculated value of f_{ref}, and the standard deviation was also much higher than in any other species. The three flap-gliding species (squares) are not clustered in any particular part of the table.

Discussion

Birds that flew slower than V_{mp}

Although it was not anticipated that any bird would fly at a speed less than the value of V_{mp} calculated for that species, the observed speeds were evenly divided below and above V_{mp}. Eight of the 16 species flew at mean speeds between 0.73 and 0.99V_{mp}, and the remaining eight species between 1.02 and 1.96V_{mp}. The mean speeds of three species were more than one standard deviation below V_{mp}. Pilots call this 'flying on the back side of the power curve', and continuous powered flight is difficult at such low speeds, both for birds and for aircraft (Pennycuick, 1997). However, three of the four species with

the lowest relative air speeds were raptors, which flew by flap-gliding. In their case, an average speed below V_{mp} is explicable, provided that the bird is capable of gliding more slowly than V_{mp}. The estimated minimum gliding speeds of the three flap-gliding species, the sparrowhawk (*Accipiter nisus*), the common buzzard (*Buteo buteo*) and the red kite (*Milvus milvus*), based on a maximum lift coefficient of 1.6, expressed as multiples of V_{mp}, were between 0.49 and 0.57. The observed average relative speeds over several flap-glide cycles were between 0.73 and 0.91. The likely explanation for the apparent anomaly of average speeds below V_{mp} is that the bird slows down during the gliding phase well below V_{mp}, but starts flapping before it approaches the minimum (stalling) speed, then accelerates while flapping to V_{mp} or a little above. Flap-gliding involves a cycle of speed changes, with a maximum speed near V_{mp} and an average speed below V_{mp}. The term 'undulating' flight for flap-gliding (as used by Rayner, 1977; Rayner, 1985) is misleading and should be avoided. The speed undulates, but the height usually does not, at least not enough to be easily discernible.

The low relative speed (0.82) observed in the mute swan (*Cygnus olor*) in flapping flight is anomalous and cannot be explained in this way. The speeds were very consistent (low standard deviation), probably because the same small group of swans was flying back and forth along the shore. A discrepancy in this direction would result if the value assumed for the induced drag factor (k=1.2) were too high, but the effect is small. The lowest possible value is k=1.0, for an improbable lossless actuator disc. This would reduce the estimate of V_{mp} from 19.4 to 18.5 m s^{-1} and raise the relative speed from 0.82 to 0.86, leaving the anomaly unresolved. These swans require a long takeoff run, and need some time and distance to accelerate to a steady flying speed, and they sometimes landed on the water near the lighthouse on a pond behind the beach. The intention was to measure their speeds only when they were flying steadily along, but it is possible that the mean speed was inadvertently biased downwards by making some observations before the swans had accelerated to V_{mp} after takeoff or when they had begun to slow down for a possible landing.

Birds that flew at speeds near or just above V_{mp}

Above the sparrowhawk (*Accipiter nisus*) in Fig. 1 are six species whose mean equivalent air speeds were within one standard deviation of the estimated V_{mp}, then four species with relative air speeds of 1.20–1.27. All these species flew by continuous flapping. There is no physical anomaly in birds flying slightly faster than V_{mp}, but the various theoretical optimum speeds proposed by Hedenström and Alerstam (Hedenström and Alerstam, 1995) would be much higher. The lowest of these is the maximum range speed (V_{mr}), at which the effective lift:drag ratio passes through a maximum. Estimates of the ratio of V_{mr} to V_{mp} for the species in the sample, calculated by Flight.bas, range from 1.60 to 1.89, but it should be noted that estimates of V_{mr} are less robust than those of V_{mp} because the value of V_{mr} depends on the exact shape of the power curve, which is poorly known. Recent physiological evidence suggests that the chemical power curve is more strongly U-shaped than Flight.bas predicts (Kvist et al., 1998). V_{mr} represents a broad peak in the effective lift:drag ratio, in a region of the power curve where the power itself is rising steeply, and the direct cost in terms of fuel energy is by no means the only consideration affecting the selection of cruising speed (Pennycuick, 1997). The results

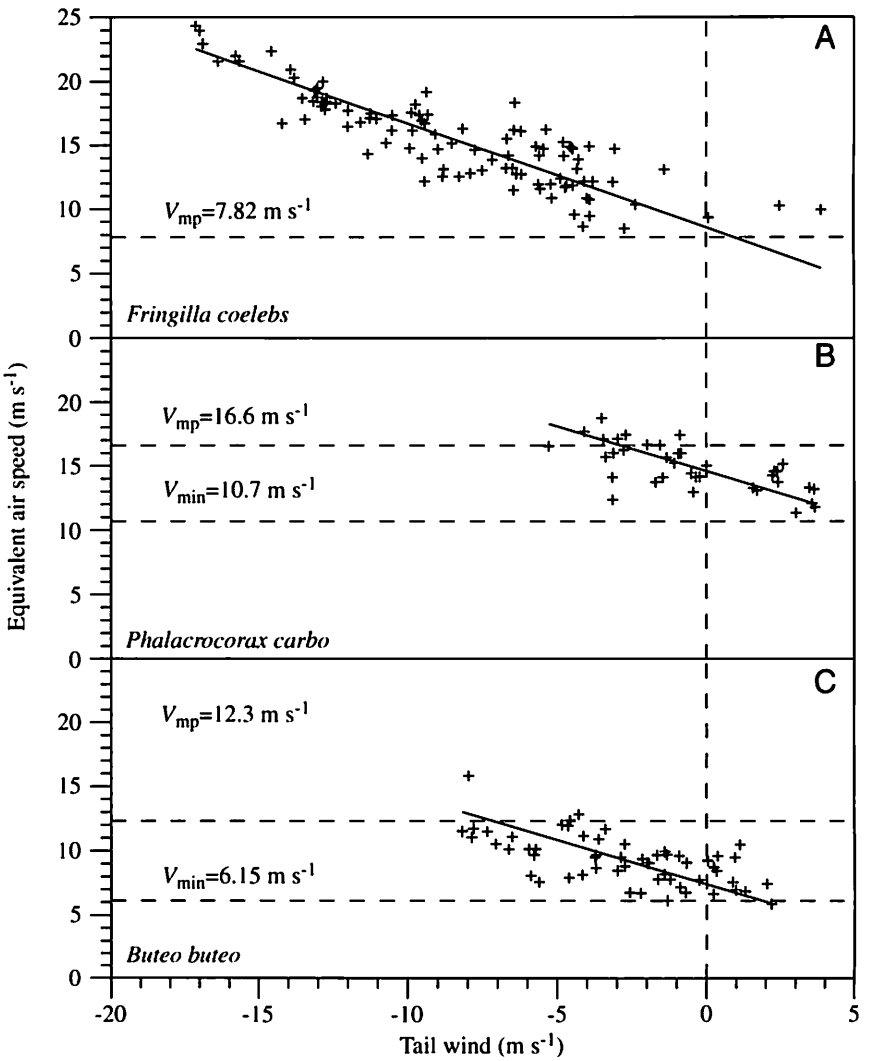

Fig. 3. Wind effect in species that flew by bounding (A), continuous flapping (B) and flap-gliding (C) with reduced major-axis lines. 'Tail wind' is the scalar difference between ground speed and air speed. Horizontal dashed lines show the minimum power speed (V_{mp}) and the minimum gliding speed (V_{min}) assuming a maximum lift coefficient of 1.6.

suggest that species cruising in steady flapping flight flew at speeds above V_{mp}, but far below V_{mr}, which is much the same pattern that was observed in earlier projects (Pennycuick, 1990; Pennycuick, 1996a), in which the birds were thought to be engaged on short local flights rather than migrating. It is possible that the same birds would cruise at higher equivalent air speeds when committed to migration at higher altitudes but, to achieve that, the true air speeds would have to be higher still (equation 5).

Birds that flew much faster than V_{mp}: bounding

Finally, the two bounding species at the top of the diagram, the starling (*Sturnus vulgaris*) and the chaffinch (*Fringilla coelebs*), flew at mean relative air speeds of 1.70 and 1.96, respectively, more than two standard deviations above V_{mp} in each case. These speeds are near the (somewhat uncertain) estimates of V_{mr} from Flight.bas for these two species. Hedenström and Alerstam (Hedenström and Alerstam, 1992) noted that migrating chaffinches and some other small species actually flew faster than their estimate for V_{mr}, but at that time they were using unduly high values of the body drag coefficient and, thus, underestimating V_{mp} and V_{mr} (see above). Fig. 3A shows that the high mean speed of the chaffinch resulted from its ability to increase speed when flying against a head wind, but Fig. 1 suggests that the two bounding species were the only ones able to do this.

The mechanical characteristics of bounding flight were identified by Lighthill (Lighthill, 1977) and further developed by Rayner (Rayner, 1977; Rayner, 1985). Bounding flight requires a cyclic variation of upward acceleration, unlike level flapping or flap-gliding flight, which do not. Fig. 4 shows a simplified bound cycle, consisting of two phases, regularly repeated, with no net change of height. In the 'ballistic phase', the bird holds its wings folded against its body, making a streamlined, fusiform shape that is assumed to generate no lift. The bird is in free fall, and the flight path curves downwards. The remainder of the cycle is the 'power phase', during which the bird flaps its wings, and the flight path curves upwards. The increase in frontal area due to wrapping the wings around the body appears to be small, and the drag in the ballistic phase is assumed to be the same as that of the body without the wings.

In continuous flapping flight, the mechanical power (P_{mech}) is represented in Flight.bas as the sum of three components, the induced power (P_{ind}), the profile power (P_{pro}) and the parasite power (P_{par}), of which the first two are functions of gravity, while the third is not:

$$P_{mech} = P_{ind}(g) + P_{pro}(g) + P_{par}. \quad (7)$$

In bounding, all three components are required during the power phase, but only the parasite power is required during the ballistic phase. The parasite power is the rate at which work is dissipated in overcoming the aerodynamic drag of the body. It does not include the work done against the component of the weight in line with the undulating flight path, which integrates to zero over a full cycle, as in a roller-coaster.

Denoting the 'power fraction', or proportion of the total

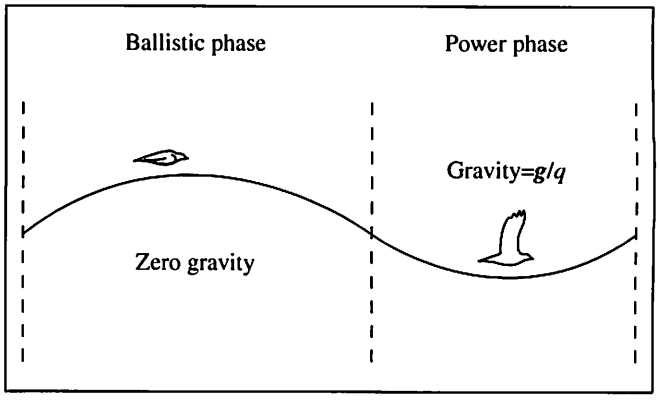

Fig. 4. Because it free-falls during the ballistic phase, a bounding bird has to pull up during the flapping phase, effectively increasing gravity (g) by a factor $1/q$, where q is the power fraction (the proportion of time spent flapping).

cycle time spent flapping, by q, the upward acceleration during the power phase has to be such as to increase the body weight by a 'load factor' equal to $1/q$ (Lighthill, 1977). In effect, the value of gravity, against which the bird has to support its weight during the power phase, is not g but g' where:

$$g' = g/q. \quad (8)$$

The induced and profile components of power, which are functions of g in level flight, become functions of g' in bounding, but are only required for a proportion q of the time. The parasite power (P_{par}) does not depend on gravity and is required all the time, whether the bird is flapping or not. The average mechanical power over the whole bound cycle is therefore:

$$P_{mech} = q[P_{ind}(g') + P_{pro}(g')] + P_{par}. \quad (9)$$

Fig. 5 shows the effect of varying the power fraction on the curves of mechanical power and effective lift:drag ratio calculated by Flight.bas for the chaffinch from the data in Table 1 and Table 3. The curves illustrate the same general conclusions that were reached by Rayner (Rayner, 1985), i.e. that the power required to fly at any given speed increases as the power fraction decreases, while the effective lift:drag ratio decreases, and also that both V_{mp} and V_{mr} shift to higher speeds as the power fraction decreases. As Rayner (Rayner, 1985) noted, bounding does not appear to confer any direct advantage in terms of either power required or distance flown per unit energy consumed.

Wingbeat frequency

As noted above, equation 2 for the reference wingbeat frequency f_{ref} is based on physical reasoning, not involving any regression coefficients or even numerical conversion factors. Nevertheless, the mean observed wingbeat frequencies, when divided by f_{ref}, gave relative wingbeat frequencies between 0.81 and 1.05 in 14 out of 16 species. f_{ref} was a benchmark calculated from a dimensional argument. Although it was not necessarily expected to predict the wingbeat frequency, Fig. 2

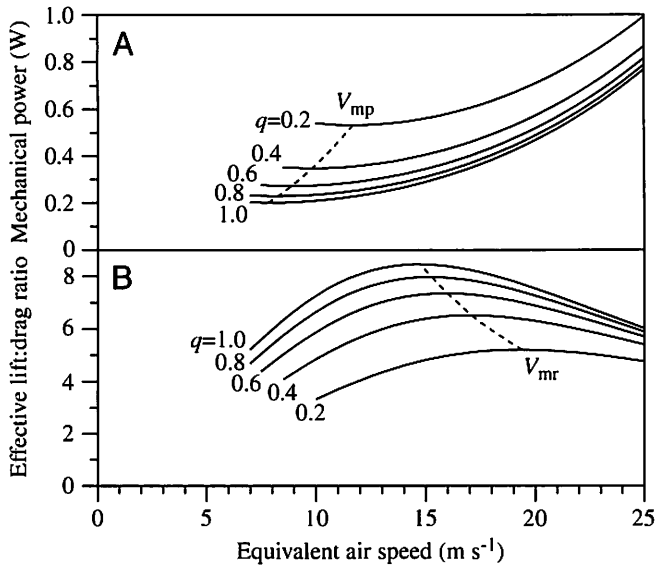

Fig. 5. Calculated curves for the chaffinch *Fringilla coelebs* of (A) mechanical power and (B) effective lift:drag ratio (based on metabolic power) for different values of the power fraction (q). These curves have been extended to 25 m s^{-1} because chaffinches were observed flying at nearly this speed, but the calculation is insecure at such high speeds.

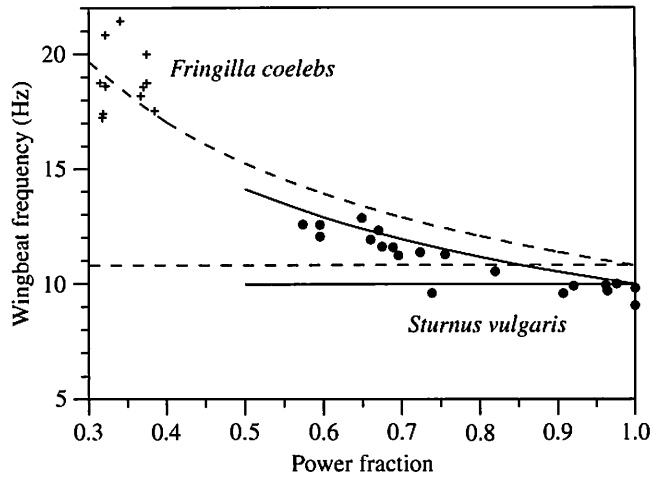

Fig. 6. Observed wingbeat frequencies in the two bounding species plotted against power fraction. Circles and solid lines, starling *Sturnus vulgaris*; crosses and dashed lines, chaffinch *Fringilla coelebs*. Curves, predicted wingbeat frequency from equation 10; horizontal lines, predicted wingbeat frequency for a power fraction of 1 (continuous flapping).

shows that actually f_{ref} did predict the wingbeat frequencies of flapping and flap-gliding species and also that the two bounding species had the highest wingbeat frequencies relative to f_{ref}. Both bounding species also showed larger standard deviations than any of the other 14 species. The observed mean equivalent frequency was within one standard deviation of f_{ref} in the case of the starling, but more than four standard deviations above in the chaffinch.

The benchmark values of f_{ref} were calculated from equation 2 using the fixed value of g in Table 3. However, wingbeat frequency was defined above as the frequency during the flapping phase of bounding (not the average frequency over a bound cycle) and it was also noted that, while the bird is pulling up in the flapping phase, the value of gravity is increased by the load factor $1/q$, where q is the power fraction. This can be expressed by modifying equation 2 in bounding (but not flap-gliding) flight to:

$$f_{ref} = m^{3/8}(g/q)^{1/2}b^{-23/24}S^{-1/3}\rho_{SL}^{-3/8}, \quad (10)$$

using g/q rather than g for gravity. This is a strong effect. The average power factor in chaffinches was 0.35, making the load factor 2.9, i.e. the chaffinches were 'pulling 2.9g' as pilots would say. This increases the wingbeat frequency, according to equation 10, by a factor of approximately $\sqrt{2.9}$, or 1.7. Power fractions in the starling ranged from 0.57 to 1.0, giving load factors between 1.8 and 1.0, and increasing the wingbeat frequency by a factor up to 1.3.

Fig. 6 shows the observed wingbeat frequencies plotted against power fraction for both the starling and the chaffinch. The curves show the wingbeat frequency predicted for each species as a function of the power fraction, from equation 10, while the horizontal lines are the predictions from equation 2, representing the hypothesis that there is no effect from the increased gravity in bounding. The ratio of the mean-square deviations of the observed frequencies from the predictions of equation 2 to that from the predictions of equation 10 was 4.99 for the starling (N=20) and 27.3 for the chaffinch (N=11). An F-test (Bailey, 1995) indicated that these variance ratios are highly significant in both cases ($P \ll 0.01$), i.e. the points in Fig. 6 are significantly closer to the curves than to the horizontal lines. Equation 10 also predicts a wingbeat frequency of 24.9 Hz from the data given by Tobalske et al. (Tobalske et al., 1999) for a zebra finch (*Taenopygia guttata*) flying in a wind tunnel with a power fraction of 0.5, which is near the middle of the range of frequencies observed. It seems that a bounding bird's wingbeat frequency does indeed respond to an increase in gravity, caused by variations of the power fraction. This is not a result that could have been anticipated by an empirical approach to the effects of gravity on wingbeat frequency.

Mass-specific work

Fig. 2 and Fig. 6 show that the wingbeat frequencies of birds in flapping and flap-gliding flight can be predicted quite well from equation 2, while the modification in equation 10 extends the prediction to bounding. Equation 2 rather than equation 10 applies to flap-gliding, because gravity is not increased in the power phase of flap-gliding, as it is in bounding. Once the wingbeat frequency can be predicted, then so also can the mass-specific work in the flight muscles (Q_m). The mass-specific work is the work done per unit mass of muscle in each contraction, and it is related to the mechanical power (P_{mech}) thus:

$$Q_m = P_{mech}/m_{musc}fq, \quad (11)$$

where f is the wingbeat frequency and m_{musc} is an estimate of

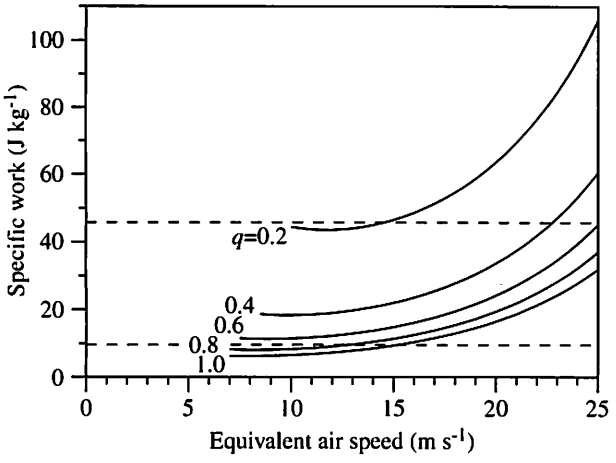

Fig. 7. Calculated curves for the chaffinch *Fringilla coelebs* of mass-specific work in the contractile component of the flight muscles for different values of the power fraction (q). Horizontal dashed lines, estimated upper and lower boundaries for 80% conversion efficiency of ATP energy into work, assuming an isometric stress of 300 kPa and strain of 0.2.

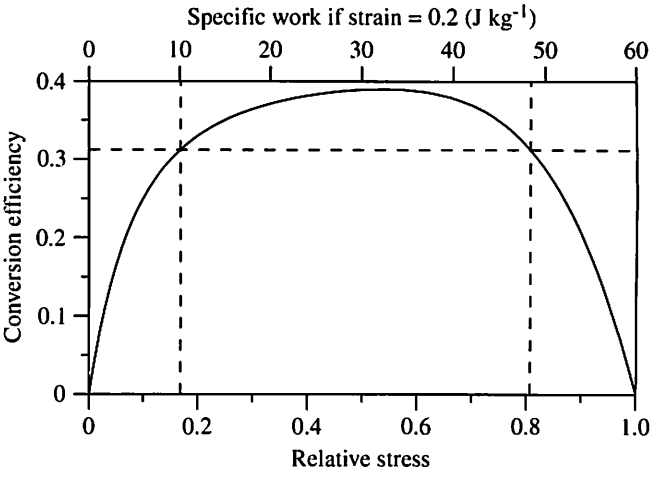

Fig. 8. Theoretical curve for efficiency of converting ATP energy into work *versus* stress normalised by dividing by the isometric stress (after Pennycuick, 1991). Vertical dashed lines, upper and lower limits of relative stress for a conversion efficiency of 80% or more of maximum. Top scale, mass-specific work assuming an isometric stress of 300 kPa and strain of 0.2.

the mass of the contractile component of the flight muscles. Equation 11 applies to continuous flapping, flap-gliding or bounding. The power fraction q appears in the denominator of equation 11 because P_{mech} is the average rate of doing work over the whole bound or flap-glide cycle, but the work is done during the power phase only.

Mass-specific work is a good variable for identifying the limits to muscular performance as it has a well defined upper limit that is not likely to vary much from one animal to another. This is not an empirical finding, but one that follows directly from the basic properties of the sliding-filament mechanism, which have been understood for many years (Huxley, 1957; McMahon, 1984). The mass-specific work is proportional to the product of the stress (s) and strain (e) in the contractile proteins, while the muscle is shortening (Pennycuick and Rezende, 1984):

$$Q_m = se/\rho_{musc}, \quad (12)$$

where ρ_{musc} is the density of muscle, usually taken to be 1060 kg m^{-3}. The stress has an upper limit that is ultimately traceable to the force that can be exerted by a single myosin filament (Pennycuick, 1992; Pennycuick, 1998). The strain also has an upper limit, related to the amount of overlap that is possible between actin and myosin filaments (White and Thorson, 1975). These upper limits may vary in different types of muscle, but are unlikely to vary much between muscles that are as similar as the flight muscles of different birds. Their actual values are difficult to measure, but that does not affect the connection with the mass-specific work. For instance, if we assume 'best-guess' values of 240 kN m^{-2} for the maximum value of the stress while the muscle is shortening (not isometric stress) and 0.20 for the maximum strain, then equation 12 gives a maximum value of approximately 45 J kg^{-1} for the mass-specific work. While this value may have to be revised in the light of future experiments, it can be used provisionally to assess the known performance of some large birds. For example, Flight.bas estimates that the mass-specific work would have to be around 36 J kg^{-1} for a very large whooper swan (*Cygnus cygnus*), whose measurements were given by Pennycuick et al. (Pennycuick et al., 1996a), to fly at V_{mp}. This particular swan was satellite-tracked as it migrated from Scotland to Iceland, and it did indeed appear to be restricted to speeds below approximately 1.3V_{mp}, landing from time to time on the water, as did other swans from the same population.

Maximum body mass in terms of specific work

Hedenström and Alerstam (Hedenström and Alerstam, 1992) also observed speeds in the region of their estimate of V_{mp} for migrating mute swans (*Cygnus olor*), combined with minimal rates of climb, and attributed this marginal flight performance to limited muscle power due to the large size of swans generally. Several known trends combine to make the specific work required to fly at V_{mp} higher in large birds than in small ones. The mechanical power required to fly increases more steeply than in direct proportion to the body mass, and one might expect that the flight muscle fraction would increase in larger birds, but apparently it does not (Greenewalt, 1962). This means that the specific power has to increase with increasing mass. The specific work increases more strongly than the specific power, because the wingbeat frequency decreases in larger birds. Estimating the mass-specific work for 150 species for which reliable (i.e. first-hand) wing measurements were available, Pennycuick (Pennycuick, 1996b) found a strong positive trend for the specific work required to fly at V_{mp}, which varied approximately with the 0.26 power of the body mass. The upper limit for Q_m was around 48 J kg^{-1}, but this estimate may be on the high side

because unduly high values, now considered obsolete (above), were used for the body drag coefficient.

Speed range

One of the reasons for the trend to higher values of the specific work in larger birds is that V_{mp} is higher in a large bird than in a small one, other things being equal. This means that it is easier for a large bird to make progress against a head wind than it is for a small one. The swans tracked by Pennycuick et al. (Pennycuick et al., 1996a) were observed flying against winds up to $20\,m\,s^{-1}$, which would require a swan to fly at 1.1 or 1.2 times V_{mp}, whereas a chaffinch flying at $20\,m\,s^{-1}$ would be flying at $2.6V_{mp}$ (Table 2). The 'speed range', defined as the ratio of the maximum level speed to V_{mp}, would appear to be more than 3 in the chaffinch (above), but is probably no more than 1.5 in any migrating swan. By having much the same flight muscle fraction as larger birds, small birds have enough 'spare' muscle power to fly at high relative speeds when a head wind makes this necessary.

Conversely, they require only a part of their available muscle power to fly at speeds near V_{mp}. When a chaffinch is not obliged to penetrate into a head wind, the specific work required from its flight muscles is very low. According to Flight.bas, it would be below $10\,J\,kg^{-1}$ at speeds up to $15\,m\,s^{-1}$ in a chaffinch that was flapping continuously (Fig. 7). This would result in inefficient conversion of fuel energy into work, for the reason shown in Fig. 8, which is a curve of the efficiency of converting ATP energy into work as a function of stress, calculated from the sliding-filament theory of Huxley (Huxley, 1957) as presented by McMahon (McMahon, 1984). The left-hand end of the curve expresses the obvious fact that, if the stress is zero, the muscle consumes fuel energy but does no work, and the efficiency is therefore also zero. The stress has to be high enough to be clear of the steeply rising part at the left-hand end of the curve, but not so high as to reach the steeply falling part at the right-hand end. According to Fig. 8, the specific work needs to be between approximately 10 and $48\,J\,kg^{-1}$ for the conversion efficiency to be above 80 % of its maximum value. Although these values are subject to some uncertainty (Pennycuick, 1991), the upper limit as shown fits quite well with the specific work calculated by Flight.bas for large birds flying at V_{mp}, and this implies that small birds would need to take some action to keep the specific work well above $10\,J\,kg^{-1}$.

Bounding and operating frequency

Three possible strategies come to mind for a small bird, flying near V_{mp}, to increase the specific work in its flight muscles without increasing the power. First, the bird might recruit only a fraction of the fibres in the flight muscles and continue to flap continuously. Second, it might use all the fibres, but flap-glide, so increasing the specific work in inverse proportion to the power fraction. Third, it might use all the fibres, but resort to bounding, in which case decreasing the power fraction would also increase the specific work, but more strongly than in flap-gliding (Fig. 7). However, Fig. 5 shows that bounding entails increased power and reduced lift:drag ratio, which would have to be offset by any gains in efficiency.

Although Fig. 7 shows that bounding is a highly effective method of adjusting the specific work over a wide range, Fig. 5 shows that bounding incurs penalties in both power and effective lift:drag ratio, whereas the other two methods do not. However, bounding increases the wingbeat frequency, and this allows the flight muscles to be adapted to a higher 'operating frequency' as defined by Pennycuick and Rezende (Pennycuick and Rezende, 1984). This means that the maximum strain rate of the myofibrils can be set to a higher value than would be possible if the muscles were adapted to operate efficiently in continuous flapping. The effect is that less muscle is needed to fly at maximum speed or, alternatively, that a given amount of muscle can handle a wider speed range without being forced to operate at unduly low values of the specific work at low speeds. Of course, it remains possible that chaffinches flying in the vicinity of V_{mr} may recruit only a part of the flight muscles, in addition to increasing the specific work by bounding.

Optimal migration

Any of the alternative hypotheses proposed by Hedenström and Alerstam (Hedenström and Alerstam, 1995) would predict that birds 'should' migrate at higher speeds than were observed in this study, except possibly in the case of the two small passerines, which flew by bounding. Even these only flew much faster than V_{mp} when flying against head winds. The first point to be established, before any theories of optimal migration can be tested, is whether the low relative speeds reported here are an artefact due to restricting observations to low-flying birds. To check that, the speeds of birds at normal altitudes for long-distance migration would need to be measured against the same benchmark (V_{mp}). This would require high-flying birds to be both tracked and identified, which presents some technical difficulties. If these could be overcome, and it turns out that cruising speeds observed at higher altitudes are still near V_{mp} as calculated by Flight.bas, the next question to be considered is whether Flight.bas consistently overestimates V_{mp}. At present, this seems unlikely in view of the wind tunnel experiments of Pennycuick et al. (Pennycuick et al., 1996b), in which good agreement was obtained between observed and calculated values of V_{mp}, following downward revision of the anomalously high values previously assumed for the body drag coefficient. The predicted V_{mp} needs to be tested on a wider range of species, bearing in mind that such measurements are sensitive to the quality of the wind tunnel environment (Pennycuick et al., 1997).

If it can be confirmed that migrants flying at higher altitudes do cruise at higher speeds, relative to the value of V_{mp} predicted by Flight.bas, then there would be a motive for attempting to calculate additional benchmark speeds, corresponding to the various optimal speeds, proposed by Hedenström and Alerstam (Hedenström and Alerstam, 1995). Of course, Flight.bas in its present form will generate power

estimates at any speed required. However, the underlying theory involves simplifications (fully explicit in the published version), which are satisfactory at speeds around V_{mp}, but are experimentally untested at higher speeds and may have to be modified in the light of future experiments. It is unclear at present what bird species (if any) have either sufficient mechanical power available from their muscles to fly at speeds much above V_{mp} or sufficient aerobic capacity for sustained cruising at such high speeds, especially at high altitudes. This needs to be established by measurements in high-quality wind tunnels of both the mechanical power output of the flight muscles and rates of fuel consumption in level flight up to the highest speeds that different birds can sustain.

I am deeply grateful to Lennart Karlsson, Sophie Ehnbom and Göran Walinder for their help during the field work and for the hospitality of the Falsterbo Bird Station. I relied on the help of local experts for identifying birds, especially Thomas Alerstam, Inga Rudebeck, Anders Hedenström, Susanne Åkesson, Mikael Rosén and Nils Kjellén. I am also most grateful to Anders Hedenström for supplying wing measurements of cormorants from the local population and to Jemima Parry-Jones for allowing me to measure the wings of a number of raptors at the National Birds of Prey Centre at Newent. The Leica Vector was bought under a recent Royal Society Research Grant, while earlier grants from the same source paid for the ornithodolite and the video camera. I am also indebted to Anders Kvist and two anonymous referees for comments on the first draft of the manuscript, in the light of which I have rewritten most of it. This paper is Publication No. 207 from the Falsterbo Bird Station.

References

Alerstam, T. (2000). Bird migration performance on the basis of flight mechanics and trigonometry. In *Biomechanics in Animal Behaviour* (ed. P. Domenici and R. W. Blake), pp. 105–124. Oxford: Bios.

Alerstam, T. and Hedenström, A. (1998). The development of bird migration theory. *J. Avian Biol.* **29**, 343–369.

Bailey, N. T. J. (1995). *Statistical Methods in Biology*. Third edition. Cambridge: Cambridge University Press.

Greenewalt, C. H. (1962). Dimensional relationships for flying animals. *Smithsonian Misc. Collns* **144**, 1–46.

Hedenström, A. and Alerstam, T. (1992). Climbing performance of migrating birds as a basis for estimating limits for fuel-carrying capacity and muscle work. *J. Exp. Biol.* **164**, 19–38.

Hedenström, A. and Alerstam, T. (1995). Optimal flight speed of birds. *Phil. Trans. R. Soc. Lond. B* **348**, 471–487.

Huxley, A. F. (1957). Muscle structure and theories of contraction. *Prog. Biophys. Biophys. Chem.* **7**, 255–318.

Karlsson, L. (1992). *Falsterbo ur Fågelperspektiv*. Falsterbo Bird Station Publication 150. 156pp.

Kvist, A., Klaassen, M. and Lindström, Å. (1998). Energy expenditure in relation to flight speed: what is the power of mass loss rate estimates? *J. Avian Biol.* **29**, 485–498.

Lighthill, J. (1977). Introduction to the scaling of aerial locomotion. In *Scale Effects in Animal Locomotion* (ed. T. J. Pedley), pp. 365–404. London: Academic Press.

McMahon, T. A. (1984). *Muscles, Reflexes and Locomotion*. Princeton, NJ: Princeton University Press.

Pennycuick, C. J. (1975). Mechanics of flight. In *Avian Biology*, vol. 5, chapter 1 (ed. D. S. Farner and J. R. King), pp. 1–75. New York: Academic Press.

Pennycuick, C. J. (1982a). The ornithodolite: an instrument for collecting large samples of bird speed measurements. *Phil. Trans. R. Soc. B* **300**, 61–73.

Pennycuick, C. J. (1982b). The flight of petrels and albatrosses (Procellariiformes), observed in South Georgia and its vicinity. *Phil. Trans. R. Soc. B* **300**, 75–106.

Pennycuick, C. J. (1989). *Bird Flight Performance. A Practical Calculation Manual*. Oxford: Oxford University Press.

Pennycuick, C. J. (1990). Predicting wingbeat frequency and wavelength of birds. *J. Exp. Biol.* **150**, 171–185.

Pennycuick, C. J. (1991). Adapting skeletal muscles to be efficient. In *Efficiency and Economy in Animal Physiology* (ed. R. W. Blake), pp. 33–42. Cambridge: Cambridge University Press.

Pennycuick, C. J. (1992). *Newton Rules Biology*. Oxford: Oxford University Press.

Pennycuick, C. J. (1996a). Wingbeat frequency of birds in steady cruising flight: new data and improved predictions. *J. Exp. Biol.* **199**, 1613–1618.

Pennycuick, C. J. (1996b). Stress and strain in the flight muscles as constraints on the evolution of flying animals. *J. Biomech.* **29**, 577–581.

Pennycuick, C. J. (1997). Actual and 'optimum' flight speeds: field data reassessed. *J. Exp. Biol.* **200**, 2355–2361.

Pennycuick, C. J. (1998). Towards an optimal strategy for bird flight research. *J. Avian Biol.* **29**, 449–457.

Pennycuick, C. J. (1999). *Measuring Birds' Wings for Flight Performance Calculations*. Second edition. Bristol: Boundary Layer Publications.

Pennycuick, C. J., Alerstam, T. and Hedenström, A. (1997). A new wind tunnel for bird flight experiments at Lund University, Sweden. *J. Exp. Biol.* **200**, 1441–1449.

Pennycuick, C. J., Einarsson, O., Bradbury, T. A. M. and Owen, M. (1996a). Migrating whooper swans (*Cygnus cygnus*): satellite tracks and flight performance calculations. *J. Avian Biol.* **27**, 118–134.

Pennycuick, C. J., Klaassen, M., Kvist, A. and Lindström, Å. (1996b). Wingbeat frequency and the body drag anomaly: wind tunnel observations on a thrush nightingale (*Luscinia luscinia*) and a teal (*Anas crecca*). *J. Exp. Biol.* **199**, 2757–2765.

Pennycuick, C. J. and Rezende, M. A. (1984). The specific power ouptut of aerobic muscle, related to the power density of mitochondria. *J. Exp. Biol.* **108**, 377–392.

Rayner, J. M. V. (1977). The intermittent flight of birds. In *Scale Effects in Animal Locomotion* (ed. T. J. Pedley), pp. 437–443. London: Academic Press.

Rayner, J. M. V. (1985). Bounding and undulating flight in birds. *J. Theor. Biol.* **117**, 47–77.

Spedding, G. R. and Pennycuick, C. J. (2001). Uncertainty calculations for theoretical power curves. *J. Theor. Biol.* **208**, 127–139.

Sutton, O. G. (1953). *Micrometeorology*. New York: McGraw Hill.

Tobalske, B. W., Peacock, W. L. and Dial, K. P. (1999). Kinematics of flap-bounding flight in the zebra finch over a wide range of speeds. *J. Exp. Biol.* **202**, 1725–1739.

White, D. C. S. and Thorson, J. (1975). *The Kinetics of Muscle Contraction*. Oxford: Pergamon.